University of Groningen

Assessment of uncertainties associated with Monte Carlo-based personalized dosimetry in clinical CT examinations

Akhavanallaf, Azadeh; Xie, Tianwu; Zaidi, Habib

Link to publication in University of Groningen/UMCG research database

PAPER

Assessment of uncertainties associated with Monte Carlo-based personalized dosimetry in clinical CT examinations

To cite this article: Azadeh Akhavanallaf *et al* 2020 *Phys. Med. Biol.* **65** 045008

View the article online for updates and enhancements.

Physics in Medicine & Biology

IPEM Institute of Physics and Engineering in Medicine

PAPER

Assessment of uncertainties associated with Monte Carlo-based personalized dosimetry in clinical CT examinations

Azadeh Akhavanallaf[1], **Tianwu Xie**[1,2] and **Habib Zaidi**[1,3,4,5,6]

1. Division of Nuclear Medicine and Molecular Imaging, Geneva University Hospital, CH-1211 Geneva 4, Switzerland
2. Institute of Radiation Medicine, Fudan University, Shanghai 200032, People's Republic of China
3. Geneva University Neurocenter, Geneva University, CH-1205 Geneva, Switzerland
4. Department of Nuclear Medicine and Molecular Imaging, University of Groningen, University Medical Center Groningen, 9700 RB Groningen, The Netherlands
5. Department of Nuclear Medicine, University of Southern Denmark, 500 Odense, Denmark
6. Author to whom any correspondence should be addressed.

E-mail: habib.zaidi@hcuge.ch

Abstract

The clinical value of x-ray computed tomography (CT) has skyrocketed in the last decade while at the same time being the main source of medical exposure to the population. Concerns regarding the potential health hazards associated with the use of ionizing radiation were raised and an appropriate estimation of absorbed dose to patients is highly desired. In this work, we aim to validate our developed Monte Carlo CT simulator using in-phantom dose measurements and further assess the impact of personalized scan-related parameters on dosimetric calculations. We developed a Monte Carlo-based CT simulator for personalized organ level dose calculations, in which the CT source model, patient-specific computational model and personalized scanning protocol were integrated. The CT simulator was benchmarked using an ionization chamber and standard CT Dose Index phantom while the dosimetry methodology was validated through experimental measurements using thermoluminescent dosimeters (TLDs) embedded within an anthropomorphic phantom. Patient-specific scan protocols extracted from CT raw data and DICOM image metadata, respectively, were fed as input into the CT simulator to calculate individualized dose profiles. Thereby, the dosimetric uncertainties associated with using different protocol-related parameters were investigated. The absolute absorbed dose difference between measurements and simulations using the ionization chamber was less than 3%. In the case of the anthropomorphic phantom, the absolute absorbed dose difference between simulations and TLD measurements ranged from −8.3% to 22%, with a mean absolute difference of 14% while the uncertainties of protocol-related input parameters introduced an extra absolute error of 15% to the simulated results compared with TLD measurements. The developed methodology can be employed for accurate estimation of organ level dose from clinical CT examinations. The validated methodology can be further developed to produce an accurate MC simulation model with a reduced computational burden.

1. Introduction

Computed tomography (CT) has become a key diagnostic imaging modality in clinical diagnosis of a wide range of diseases. The number of CT scans in the US had an average annual increase of 10% between 1995 and 2015 (IMV Publishing 2018, Ferrero *et al* 2019). The sharp utilization trend of CT imaging in clinical setting has raised health concerns regarding potential risks of ionizing radiation on patients undergoing CT examinations. Although medical exposure brings individual benefits to the patient, it should still follow the principles of justification and optimization (De González *et al* 2009, Sodickson *et al* 2009). In this context, each medical radiological procedure has to be optimized for the specific task and individual patient. Efforts devoted to designing patient-specific CT

scanning protocols depending on the target task, scanner model and patient anatomy, can greatly benefit from a unified methodology for radiation dose estimation (Lahham and ALMasri 2018, Xie *et al* 2019).

Direct measurement of energy deposition in the different tissues/organs within the patient's body is not conceivable in a clinical setting. Therefore, experimental measurements using dosimeters embedded within physical phantoms and Monte Carlo simulations using realistic anthropomorphic computational phantoms served as substitutes. Monte Carlo simulation, deemed to be the gold standard technique for dosimetry calculations, should be carefully validated against experimental measurements because the input parameters related to the imaging system, patient's anatomical model and the scanning protocol dictate the accuracy of the obtained results. A number of studies reported on the use of Monte Carlo programs benchmarked using standard CT Dose Index (CTDI) and other anthropomorphic physical phantoms (DeMarco *et al* 2005, Deak *et al* 2008, Li *et al* 2011a, Long *et al* 2013). The paradigm shift introduced by advances in personalized medicine and precision medicine stimulated the development of strategies for patient-specific dosimetry and protocol optimization during the last few years. In this context, Segars *et al* constructed personalized computational models by mapping the segmented model of patient CT images to a template anatomical model using a deformable registration algorithm (Segars *et al* 2009). Li *et al* developed a Monte Carlo code for patient-specific dose calculation (Li *et al* 2011b) by constructing patient-specific computational models through manual segmentation that are fed as input to the Monte Carlo program. Kalender *et al* constructed personalized whole-body phantoms from regional CT images through appending the scan range to an anchor phantom to assess the effect of scatter and overscanning on organ doses (Kalender *et al* 2014). Xie *et al* proposed a methodology for constructing patient-specific computational models based on deformable registration of patient CT regional images on a habitus-dependent anchor phantom (Xie *et al* 2018, Xie and Zaidi 2019). They employed the structural deformation of the best-fitting phantom from a previously developed library of computational models through automated non-rigid registration to estimate the patient-specific model (Akhavanallaf *et al* 2019). They calculated patient's organ-level radiation dose using the obtained personalized computational phantom and imaging protocol implemented into the MC simulation. The Radimetrics™ commercial dose tracking software (Bayer HealthCare, Berlin, Germany) provides Monte Carlo-based organ-level dose profile from patient CT images where the scan parameters are extracted from CT image DICOM header information (Bayer HealthCare). Radimetrics™ simply maps the patient's regional CT images on Cristy & Eckerman mathematical computational phantoms categorized by age and gender (Cristy and Eckerman 1987). It further adjusts the phantom's diameter according to the effective diameter of the patient obtained from CT images.
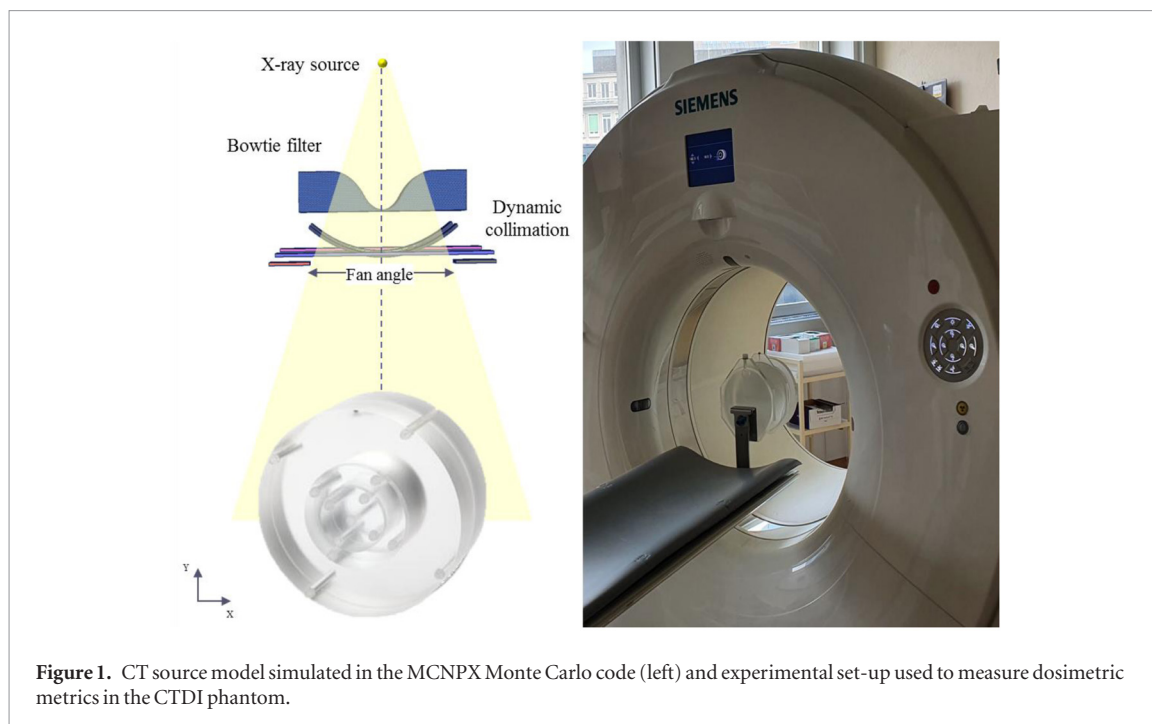
The dosimetric impact of scan parameters (e.g. x-ray energy spectrum, beam filtration, tube current modulation, tube start angle, over-ranging …) fed into Monte Carlo simulations has been investigated in previous studies (Chen *et al* 2012, Bostani *et al* 2014, Fujii *et al* 2017, Hardy *et al* 2018) and more comprehensively in the recent AAPM report No. 246 (AAPM 2019). The input data are commonly provided by CT scanner manufacturers, experimental measurements, or extracted directly from scanner control console or the generated radiation dose structured report after the examination. However, there are uncertainties associated with all sources of input parameters. Muryn *et al* examined the impact of deviations related to the input parameters on the simulated dose profiles (Muryn *et al* 2017). They studied the parameters linked to the CT scanner (e.g. x-ray spectrum, beam filtration, beam width) and the scan setup (e.g. tube start angle, scan length, isocenter position) to address the uncertainties introduced on the simulated dose when the input parameters deviate from the actual values. However, in this work, the tube current modulation and the impact of patient's anatomy were not taken into account. Lee *et al* performed organ-level dose estimation for a large cohort of CT examinations to investigate the dosimetric impact of uncertainties on patient-related and empirical scan-related parameters (Lee *et al* 2018).

In this work, we aimed to provide a computationally-efficient framework for accurate patient-specific dose estimation. To this end, we developed a unified methodology for patient-specific dosimetry from CT examinations. Unlike previous works requiring manual segmentation of CT images to construct patient-specific computational model, we adopted methodology that automatically builds patient-specific computational models from CT images. Subsequently, the validated CT source model, patient-specific computational phantom and scan parameters were integrated in the Monte Carlo code to calculate organ-level absorbed dose. Therefore, the dosimetry results were benchmarked against experimental measurements. To further assess the impact of uncertainties associated with simulation input parameters on the organ level personalized dosimetry, we compared different scenarios where the patient-specific scan-related parameters were extracted from the CT image DICOM header file and more detailed CT raw data, respectively.

2. Materials and methods

2.1. Monte Carlo simulations
In Monte Carlo-based CT dosimetry studies, three essential components are incorporated into the simulations. This includes the CT source model, computational phantom and protocol-related parameters. CT data were

Figure 1. CT source model simulated in the MCNPX Monte Carlo code (left) and experimental set-up used to measure dosimetric metrics in the CTDI phantom.

acquired on the Somatom Definition Edge scanner (Siemens Healthcare, Erlangen, Germany). The geometry of the CT system was realistically modelled by using an x-ray energy spectrum generated using SpekCalc (Poludniowski *et al* 2009) and tuning the inherent filtration of the scanner's x-ray tube and half value layer (HVL) associated with the x-ray energy. The applied inherent filtration and HVL were extracted from system owner manual (Siemens AG 2012) and were matched with the results reported by Yang *et al* (2017). The Bowtie or shaped filter and beam collimators, including dynamic collimators as well as fixed collimation components were elaborately modelled based on the information provided by the manufacturer. The geometry of the gantry (e.g. focal spot size, the distance between focal spot and isocenter), fan angle, etc. were taken into account in the simulation as shown in figure 1. This CT source model was created within the MCNPX general purpose Monte Carlo radiation transport code (version 2.6) (Waters 2002). The computational phantom with its detailed anatomy was constructed using a previously developed methology based on automated registration of the patient's CT images to an anchor phantom (Xie *et al* 2019). The protocol-related parameters, including scan mode, tube potential, total beam collimation, revolution time, exposure time, table speed, pitch factor and tube current modulation were extracted from DICOM header information using a MATLAB (The MathWorks Inc., Natick, MA, USA) function and implemented in the simulation code. The tube current modulation (longitudinal and angular), tube start angle and over-ranging information were extracted from the DICOM header information of both CT images and CT raw data and used in the simulation setup.

2.2. Validation of the CT scanner model

The conversion of the relative MCNPX dose tallies to absolute dose value was performed by conducting free in air measurement using a 10 cm RaySafe™ Solo pencil ionization chamber (Unfors RaySafe GmbH, Germany). The ionization chamber was placed at the isocenter of the CT scanner with its active volume aligned with the axis of gantry rotation. Free in air measurements were performed in single axial scans where the absorbed dose derived from simulations was calculated as:

$$D_{estimated} = D_{simulated} \times N \times \Omega \times mAs \times CF \qquad (1)$$

where $D_{simulated}$ is the simulated absorbed dose per photon emitted from the source (F6 tally in unit of MeV/g); N is the number of photons emitted from the source per solid angle per mAs; Ω is the solid angle of the fan-beam; mAs is the effective tube current-time product value; and CF is a calibration factor to correct for uncertainties introduced in Monte Carlo simulations to calculate the absorbed dose values from simulations in absolute units of mGy. To validate the developed CT source model, we benchmarked our simulation results against standard CTDI phantom measurement for both head (16 cm diameter) and body (32 cm diameter) cylindrical phantoms. To this end, firstly, we performed free in air measurements to estimate the CF as the ratio of the absolute measured dose to the simulated dose. In equation (1), there is a linear relationship between the measured dose and mAs, which is regularly checked during routine CT scanner quality control procedures. While the factors N and Ω depend on tube potential and total collimation, respectively, the relationship between these factors and the absorbed dose is not ideally linear (Siemens AG 2012). For this reason, we reduced equation (1)
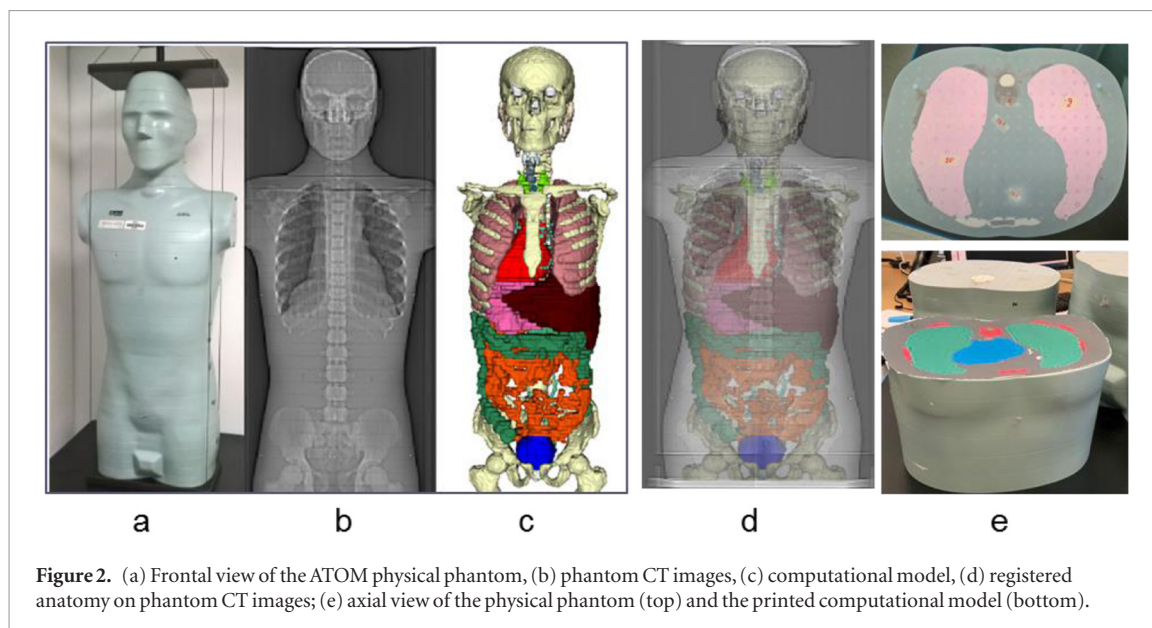
Figure 2. (a) Frontal view of the ATOM physical phantom, (b) phantom CT images, (c) computational model, (d) registered anatomy on phantom CT images; (e) axial view of the physical phantom (top) and the printed computational model (bottom).

to $D_{estimated} = D_{simulated} \times mAs \times CF$ by providing a unique calibration factor associated with the specific acquisition parameters (e.g. tube potential and total beam collimation) during CT examinations. Consequently, we measured the absolute dose in the CTDI phantom in helical mode with the same acquisition parameters used for free in air experiment to compare the simulation results against the measurements using the estimated calibration factor. Three million photons were used in this simulation to achieve a statistical error less than 2%.

2.3. Anthropomorphic phantom dose measurements

To benchmark the accuracy of the developed Monte Carlo code for patient-specific dosimetry, absorbed doses were measured in the CIRS ATOM® dosimetry verification phantom (CIRS, Inc., Norfolk, VA, USA). This anthropomorphic physical phantom, axially sliced in 25 mm thick, consists of three types of materials, including skeleton, lung and soft tissue. The physical phantom was matched to its corresponding computational twin where the boundaries of all internal organs were mapped on the physical slice consistent with their delineation in the corresponding computational model (figure 2). We used the previously developed program to construct the patient-specific phantom from CT images through automated deformable registration (Xie *et al* 2019). CT images of the ATOM phantom were employed to provide the anatomical masks of the skeleton, the lungs and body contour which constitute the basis of information used by the registration algorithm. Hence, the computational model of the phantom with detailed anatomy was constructed using the automated deformable registration algorithm.

TLDs (LiF, Harshaw TLD-100) in the form of $3.2 \times 3.2 \times 0.9 \, mm^3$ chips were inserted within the tissue equivalent dosimeter holders embedded within the phantom. TLDs were individually calibrated in terms of absorbed dose in water for Co-60 radiation. A correction factor was multiplied by the TLD results to account for the TLDs response for the specific beam quality, i.e. x-ray energy and half value layer of the beam. A total number of 103 TLDs were distributed in the phantom. Depending on the size of organs, from two to several measurement points were used enabling accurate volume-averaged organ dose calculation. The background noise was determined using separate dosimeters that were not exposed. The measured quantity from reading the TLDs is the absorbed dose in water. Calculation of the absorbed dose in other tissues involved application of a correction factor, calculated as the ratio of the average mass energy absorption coefficients in the tissue in question per mass energy absorption in water. The average of the TLD readings for each organ was used as the measured organ absorbed dose.

2.4. Patient-specific organ-level dose simulation

Validation of the developed methodology in estimating patient-specific organ-level doses from CT examinations involved the comparison of simulation results with experimental measurements using the anthropomorphic physical phantom. The CT source model, computational model and scan parameters extracted from DICOM headers of both CT images and CT raw data were integrated in the MCNPX code. The acquisition parameters, including tube voltage, total collimation width, table speed, revolution time, pitch factor, and modulated tube current, start angle and over-ranging length were modelled in this simulation setup. To simulate helical whole body scanning (90 cm length), Monte Carlo simulations were run for 16 854 discrete source positions (576 source positions per rotation) taking into account the complete tube current modulation (longitudinal and angular

modulation). Considering the linearity of the radiation output or measured dose with the mAs, the obtained energy deposition tally (Gy/particle) was multiplied by the mAs in each simulation point. To calculate organ doses in absolute units of mGy, the unique calibration factor that depends on the beam energy spectrum, filtration, and beam collimation was used. To calculate the specific calibration factor associated with the conducted CT examination, the value representing scan-specific radiation output ($CTDI_{vol}$) was simulated according to the 21 CFR 1020.33 guidelines (Bauhs *et al* 2008). Thereby, the scan-specific calibration factor was defined as the ratio of the simulated $CTDI_{vol}$ to the $CTDI_{vol}$ appearing in the dose report of anthropomorphic phantom CT examination. To evaluate the effect of dynamic collimation on dosimetric results, a correction factor defined as the time-weighted average of collimator during the scan, divided by the nominal collimator width for the scan was applied to the simulation results. The absorbed radiation dose associated with the topogram scan was also added to the simulation results.

To evaluate the accuracy of the developed simulation framework, organ-level dose profiles obtained from experimental TLD measurements were compared with simulation results as well as the doses reported by Radi-metrics™ commercial dose tracking software.

2.5. Uncertainties associated with simulation input parameters

The accuracy of results obtained from Monte Carlo radiation transport simulations depends directly on the input parameters fed into the simulator. In this section, we estimated organ-level doses using the information extracted from DICOM header information of CT images, referred to as image-based simulation, which basically contains longitudinal tube current modulation and lacks information about tube start angle and over-ranging length. In the exact simulation where the detailed input parameters were obtained from CT raw data, the angular component has been also taken into account in addition to the longitudinal tube current modulation. The complete tube current modulation was obtained from CT raw data based on CAREDose4D module in the Siemens CT scanner, which employs patient size information from the CT localizer scout scan to predict the longitudinal and angular modulation functions. Overall, the tube current value reported in the DICOM header at each table position is calculated from the moving average of complete tube current over one rotation while the high frequency components (i.e. angular modulation) are smoothed (figure 3). To simulate a helical scan in the image-based simulation, the source positions were modelled based on fixed intervals in the *Z* direction, while the angular position was determined according to the gantry revolution time and table speed obtained from the DICOM header information. However, it has been reported that over-ranging length is around half of the collimation width. This parameter is proprietary information for the different manufacturers (Schilham *et al* 2010). Therefore, we extracted over-ranging length from CT raw data to accurately simulate this feature. In the image-based simulation, the random start angle was modelled and the over-ranging length was ignored. Here, the dosimetric impact of the tube start angle and number of simulation points across the entire scan was investigated and the results compared with those obtained from exact simulations.

2.6. Statistical analysis

The comparison between the results obtained from exact simulations and experimental measurements using TLDs, serving as reference, underwent statistical analysis. Furthermore, the intraclass correlation coefficient (ICC), as a measure of the reliability of organ dose calculation methods, was considered.

3. Results

3.1. Validation of Monte Carlo simulation model

The CT source model was defined in the MCNPX code based on information provided by manufacturer by combining simple geometries. The model was validated through comparison with experimental measurements using the standard CTDI head and body phantoms. The acquisition parameters associated with the examination and the corresponding calibration factors obtained from free in air measurements are illustrated in table 1. Table 2 summarizes the central and peripheral $CTDI_{100}$ and $CTDI_{vol}$ for the protocols specified in table 1 demonstrating absolute mean differences between simulations and measurements around 6.4%. The computational model of the ATOM physical phantom derived from CT images is shown in figure 2. To validate the developed methodology for patient-specific organ-level dosimetry, the experimental CT acquisition illustrated in table 1 using the physical phantom was performed ($CTDI_{vol} = 4.97$ mGy). The results from the in-phantom measurements were considered as reference and compared with simulation results as well as organ dose profiles reported by Radimetrics™ software. The mean absolute difference between TLD measurements and MC simulations is about 14% (range [−8.3% to 22%]), while it exceeds 33% for Radimetrics™ (figure 4). The effective dose obtained from TLD measurements was about 11.44 mSv while the effective dose calculated from simulation and Radimetrics™ was about 12.44 mSv and 7.35 mSv, respectively.
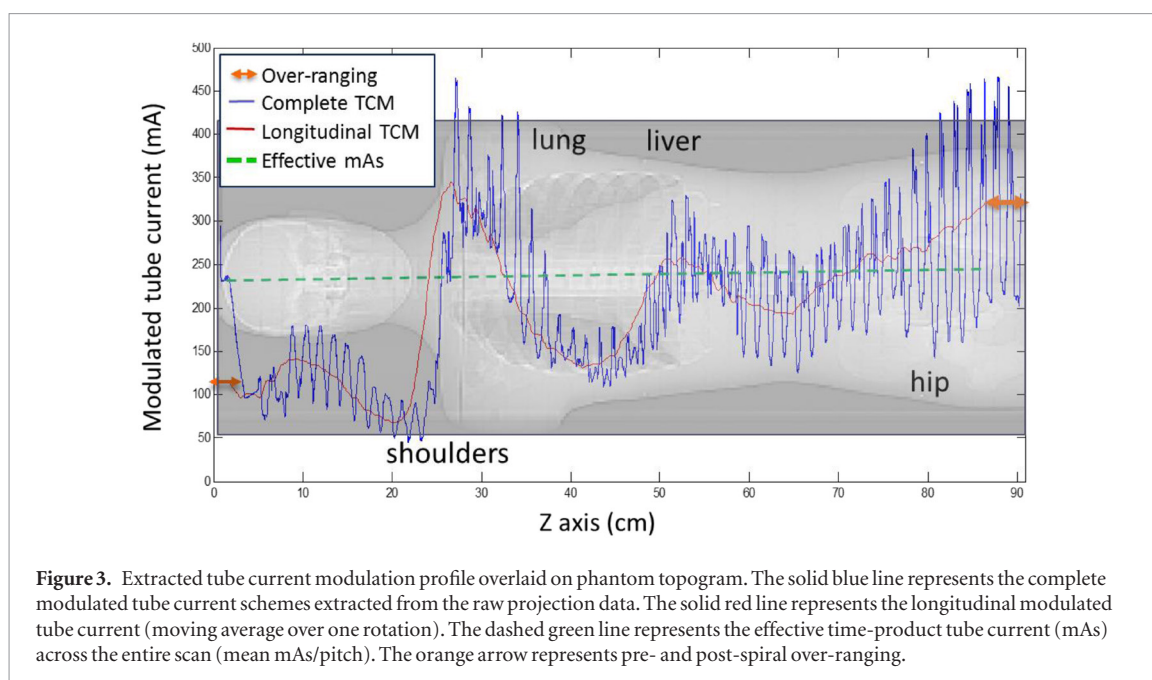
Figure 3. Extracted tube current modulation profile overlaid on phantom topogram. The solid blue line represents the complete modulated tube current schemes extracted from the raw projection data. The solid red line represents the longitudinal modulated tube current (moving average over one rotation). The dashed green line represents the effective time-product tube current (mAs) across the entire scan (mean mAs/pitch). The orange arrow represents pre- and post-spiral over-ranging.

Table 1. CT acquisition parameters for experimental measurements performed in the CTDI phantoms and the anthropomorphic physical phantom.

Acquisition parameters	Head standard (perfusion)	Head standard	Body standard	Physical phantom (whole-body)
Tube voltage (KeV)	80	120	120	100 KeV
Total collimation (mm)	64 * 0.6	12 * 1.2	64 * 0.6	64 * 0.6
Tube current (mA)	200	350	252 (ref)/210 (eff)	268 (ref)/126 (eff)
Rotation time (sec)	1	1	0.5	0.5
Pitch factor	—	—	—	0.8
Mode	Axial	Axial	Axial	Helical
Calibration factor	25.3	67.7	48.7	77.6

Table 2. Comparison between measured and Monte Carlo-based calculations of the CTDI_{100}^{C} (central), CTDI_{100}^{P} (peripheral) and $\mathrm{CTDI}_{\mathrm{vol}}$ in body and head CT dosimetry phantoms.

		Measurements			Simulations			
Acquisition type	Voltage (KeV)	CTDI_{100}^{C} (mGy)	CTDI_{100}^{P} (mGy)	$\mathrm{CTDI}_{\mathrm{vol}}$ (mGy)	CTDI_{100}^{C} (mGy)	CTDI_{100}^{P} (mGy)	$\mathrm{CTDI}_{\mathrm{vol}}$ (mGy)	$\mathrm{CTDI}_{\mathrm{vol}}$ Difference (%)
Head standard (perfusion)	80	8.39	8.94	8.76	7.68	8.47	8.21	6.3
	100	16.95	17.61	17.39	14.95	17.57	16.70	4.0
Body standard	120	7.88	14.71	12.43	6.91	17.53	13.99	12.5
Head standard	120	7.14	7.34	7.28	7.25	7.62	7.5	3.0

3.2. Uncertainties associated with input parameters

To assess the impact of input parameters on the simulation results, we obtained the input data from two sources: CT raw data and DICOM header. The complete tube current modulation obtained from CT raw data was compared with longitudinal tube current modulation obtained from DICOM header (figure 3). The organ dose resulted from image-based simulation was compared with reference values and results from exact simulation. In figure 5, the mean absolute difference between the absorbed dose from the image-based simulation compared with reference organ dose values is about 29%. The effective dose from the image-based simulation was calculated about 11.68 mSv.

To illustrate the dosimetric impact of tube start angle parameter on the simulation results, figure 5 shows the results from energy deposition tally over one complete rotation around the concerned organs. The absolute difference of the total deposited energy for the thyroid between simulation results based on exact tube start angle compared with those produced using 90° and 180° deviated start angle is about 137% and 27.5%, respectively. For the liver, this difference reduces to 26% and 23%, respectively.
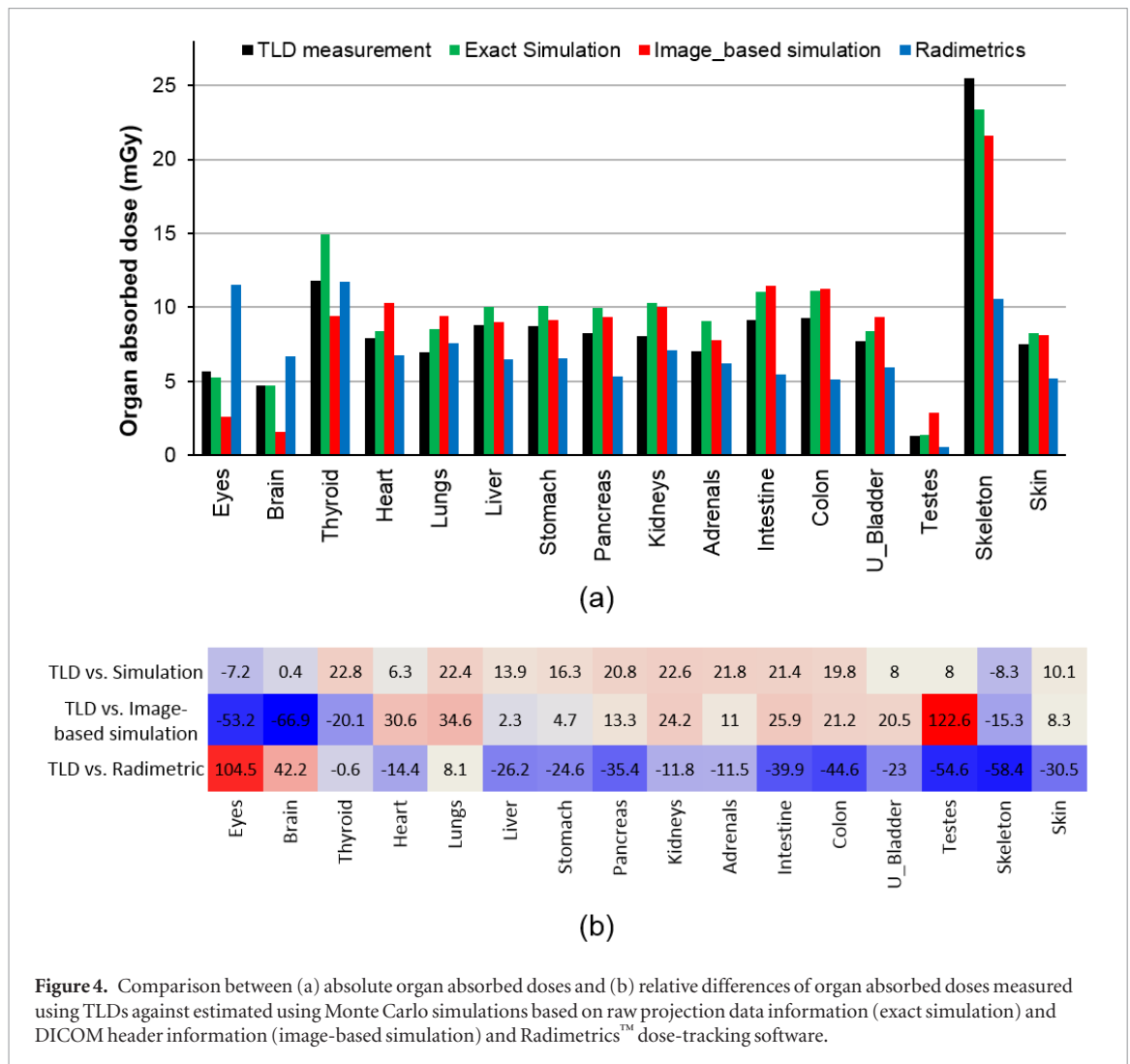
Figure 4. Comparison between (a) absolute organ absorbed doses and (b) relative differences of organ absorbed doses measured using TLDs against estimated using Monte Carlo simulations based on raw projection data information (exact simulation) and DICOM header information (image-based simulation) and Radimetrics™ dose-tracking software.
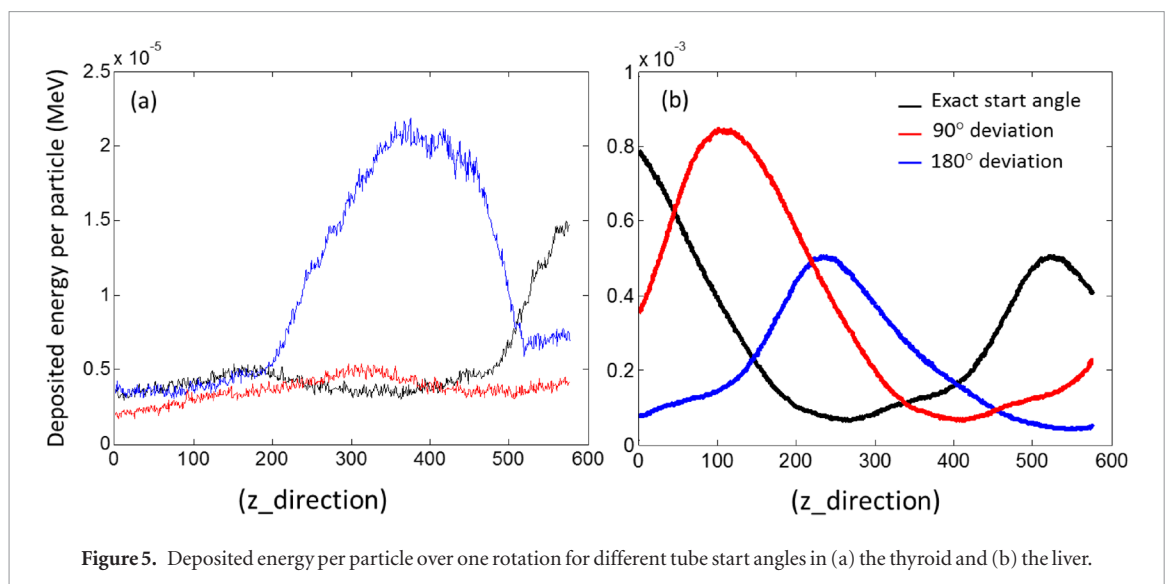

Figure 5. Deposited energy per particle over one rotation for different tube start angles in (a) the thyroid and (b) the liver.

The sources of uncertainties in organ dose simulation studied in this work originated from tube current modulation, tube start angle and the number of simulation points. To investigate the dosimetric impact of these factors, organ doses obtained from different simulation scenarios were compared against exact simulations in terms of percent difference, illustrated in figure 6. By implementing only the longitudinal modulation scheme to the simulated dose values the absolute mean difference compared to the organ doses resulted from exact simulation was about 3.9% while the absolute difference for small peripheral organs like thyroid and testis exceeds 10% and 13 %, respectively. By implementing the reported effective time product tube current as a fixed tube current

Figure 6. Heat map displaying the relative differences between organ absorbed doses obtained from exact Monte Carlo simulations (information extracted from raw projection data) and image-based simulations (information extracted from CT image DICOM header information) considering longitudinal tube current modulation, fixed tube current (effective mAs), simulation point intervals in *Z* direction (2 mm, 6 mm and 10 mm) and start angle deviation from the actual angle (50°, 90° and 180°).

into the simulation, the absolute mean difference of estimated organ doses against exact simulation was calculated about 15.15% while it exceed 50% for brain and eye lenses. The dosimetric impact of the number of simulation points on the organ doses was investigated by modelling the different simulation intervals in the *z*-direction where the projection angles were conserved according to the exact tube start angle and fixed table speed. The absolute mean difference between the results from exact simulation compared to 2 mm interval, 6 mm interval and 10 mm interval is about 11.5, 11.45 and 13%. The mean absolute difference between exact simulation against approximate ones starting at 50°, 90° and 180° with 2 mm interval of simulation points in z direction is about 12%, 13.8% and 14%, respectively.

3.3. Statistical analysis

The differences between experimental measurements using TLDs and exact simulations were not statistically significant (*P*-value = 0.53). The ICC showed that the results obtained from exact simulations are in excellent agreement with experimental measurements with a consistency of 0.98 and absolute agreement of 0.97.

4. Discussion

We developed a Monte Carlo framework for radiation dose assessment from CT examinations toward patient-specific organ-level dose monitoring. To this end, we integrated a CT source model, computational anthropomorphic phantom and protocol parameters into a dedicated Monte Carlo program. Experimental measurements using an ionization chamber and TLD chips were performed to validate the developed methodology. Considering the dependency of the calibration factor on CT acquisition parameters, we calculated, for each scenario, a unique calibration factor associated with scan-specific parameters. Since the CTDI$_{vol}$ index represents the radiation output of a specific CT scan, we used this value to benchmark the developed CT source model. The calibration factor was determined as the ratio of the reported CTDI$_{vol}$ on the scanner control console and CTDI$_{vol}$ obtained from simulation. Furthermore, it has been previously reported that the variation of organ doses obtained from scanner-specific simulations across different scanner manufacturers are close to the variation in scanner-specific CTDI$_{vol}$ (Turner *et al* 2010). In this context, calculation of a unique calibration factor associated with a specific CT examination (scanner-specific and scan-specific) enables to utilize our Monte Carlo program for a variety of protocols and scanner models.

A reasonable agreement was observed between experimental in-phantom measurements and Monte Carlo simulations in organ-level dosimetry. The TLD results had an uncertainty of 7% where standard dosimeter

calibration, background noise subtraction, and response correction for specific energy range of x-ray beams has been taken into account. Likewise, there is a statistical uncertainty associated with Monte Carlo simulation results, estimated to be less than 2% for all simulations carried out in this work. The simulated organ doses over-estimated the measured ones in most of the cases. These deviations are mainly caused by the differences between the constructed computational model and the actual physical phantom employed for measurements. These errors are partly caused by the registration process between the computational model and the physical phantom, partly related to differences in terms of material composition, since the physical phantom is made of three different tissue equivalent materials (bone, lung, and soft tissue), while the elemental compositions of the different organs have been implemented into the simulations according to the ICRP report 89 (ICRP 2002). For skeleton dose measurements, most of the TLDs were inserted in the spinal cord while in simulations all bones contributed to skeleton dose, resulting in 8.3% underestimation. Radimetrics™ software underestimated organ doses compared to TLD measurements by a mean absolute difference of 26% for most organs, except the brain and eyes. A slight misalignment of CT images of the physical phantom with the stylized phantom used by Radimetrics™ was observed in the head region, which explains the overestimation of the absorbed dose to these two organs by about 73%. However, the physical phantom utilized in this work is anthropomorphically similar to the reference man computational phantom, whereas the stylized computational phantom used by Radimetrics™ does not reflect the anatomical features of this model. Radimetrics™ provides a simple protocol-based registration of CT scan localizer or topogram to predefined anatomical landmarks in the stylized phantom without resorting to any form of deformable registration. The acquisition parameters that Radimetrics™ used in this simulation were extracted from DICOM header information and may introduce extra errors to the results. Therefore, the results presented in figure 4 confirm the good agreement between exact simulations and experimental measurements (within the range [−8.3% to 22%]). The differences between estimated organ doses obtained from TLD measurements and exact simulations were not statistically significant (*P*-value = 0.53).

The accuracy of organ dose estimation is directly dependent on the accuracy of the constructed computational model representing patient's anatomy and the modelling of exposure conditions (AAPM 2019). The uncertainty associated with the construction of patient-specific computational phantoms was investigated in our previous study, where the mean absolute differences between organ doses estimated from a reference model (manual segmentation) and those estimated from the constructed patient-specific model were within the range [0.5%–29%] with a mean value of 9.1% (Xie *et al* 2019). In this work, we further analysed the organ dose uncertainties associated with irradiation conditions. In this context, the patient's dose profile calculated from exact simulations (input parameters obtained from raw CT projection data) against image-based simulations (input parameters derived from DICOM header of CT images) was investigated. The extra errors introduced to the simulation results caused by the smoothed tube current modulation, lack of knowledge about tube start angle and ignoring the overranging distance were considered. In the exact simulations, we simulated 16 854 projection points where the mAs values were known for each point. For the image-based simulation, the number of simulation points was determined based on the intervals in the *Z* direction (scan length/*Z*-interval) and the mAs values were reported in each axial slice of CT images. According to figure 6, using only longitudinal current modulation introduces an extra error within the range [−10% to 13%] (mean = 3.85%) to the simulation results. The value of total tube current time product of the examination obtained from CT raw data is 6.6% higher than that calculated from CT DICOM images owing to the smoothing of the angular current modulation. As seen in figure 6, there are substantial differences between organ doses produced by exact simulations and the results based on the deviated tube starting angles within the range [−22% to 110%]. The impact of tube start angle on the calculated doses for small and superficial organs (e.g. thyroid and testes) is significant. The overranging length and dynamic collimation was modelled in this simulation. The dose efficiency of dynamic collimation has been reported to be in the range of 90% in case of full beam collimation on Siemens CT scanners, which significantly reduces the dosimetric impact of overranging (Siemens AG 2012). The impact of the number of simulation points on organ doses was investigated in the condition where the start angle was exactly modelled according to the information extracted from CT raw data and accordingly the angular positions of the simulated source points were exactly matched to the exact simulations scenario. By increasing the simulation intervals in the z-direction, the uncertainty for estimation of the organ dose slightly increases. However, the difference between 2 mm interval and 6 mm interval does not show any significant impact on the dosimetric results. For large organs, the impact of simulation parameters on organ absorbed doses is less than that for small organs like the testis and thyroid. Since Monte Carlo simulations provide the mean deposited energy per particle for a specific source position, organ absorbed doses are calculated based on the summation of the deposited energy multiplied by the tube current time product for all simulated source positions. Therefore, it is expected that for large organs, the simulation parameters are compensated during this summation while for small organs or partially irradiated organs in the border of CT examination, the simulation parameters play important roles in organ level dosimetry. We also anticipate improved modelling accuracy using the new version of MCNP code (version 6.2).

This study bears a number of inherent limitations. First, the experimental measurements using the anthropomorphic phantom were performed only once using a limited number of TLDs, which might introduce some statistical uncertainties. Second, this study is limited to a single CT scanner and a single set of acquisition parameters. Third, a single physical phantom (adult male) was studied while it can be extended to other categories, e.g. female and paediatrics. Lastly, the personalized computational model was constructed using deformable registration where the uncertainties associated with the registration algorithm introduced some extra errors to the simulation results. Thanks to advances in deep learning algorithms, patient-specific dosimetry is becoming feasible in the clinic. Using deep neural network algorithms, patient-specific computational models can be constructed from CT images through automated segmentation (Xie and Zaidi 2019, Zhang *et al* 2019). Furthermore, the dose map of an individual patient commonly obtained from computationally expensive Monte Carlo simulations can be directly generated through deep learning approaches (Lee *et al* 2019).

5. Conclusion

An experimental setup was performed in this work to evaluate the accuracy of Monte Carlo-based personalized organ-level dosimetry from CT examinations. Individual patient dose profiles can be accurately estimated using the developed simulation framework. Investigations considering different CT scanners and scanning protocols can be conducted to optimize CT technologies and scanning protocols. The validated CT scanner model could be employed in personalized CT dosimetry where the patient-specific computational model is constructed using different approaches. We also assessed the dosimetric impact of input parameters in organ-level dose simulation. It can be concluded that, when the information from the CT raw projection data is not available, the simulation results could be acceptable if the input parameters obtained from CT image DICOM header are correctly employed in the simulation setup. In this context, the longitudinal tube current modulation should be implemented at least by averaging simulations with three random tube start angles. The number of simulation points should be defined appropriately in the *Z* direction and in case of dynamic collimation, over-ranging length can be ignored. Hence, the methodology can be further expanded to produce an accurate MC simulation toolkit with a reduced computational burden.

Acknowledgments

ORCID iDs

Tianwu Xie ⓘ https://orcid.org/0000-0003-3447-7707
Habib Zaidi ⓘ https://orcid.org/0000-0001-7559-5297

References

AAPM 2019 *Report No. 246—Estimating Patient Organ Dose with Computed Tomography: a Review of Present Methodology and Required DICOM Information* (Alexandria, VA: American Association of Physicists in Medicine)

Akhavanallaf A, Xie T and Zaidi H 2019 Development of a library of adult computational phantoms based on anthropometric indexes *IEEE Trans. Radiat. Plasma Med. Sci.* **3** 65–75

Bauhs J A, Vrieze T J, Primak A N, Bruesewitz M R and McCollough C H 2008 CT dosimetry: comparison of measurement techniques and devices *Radiographics* **28** 245–53

Bayer HealthCare Radimetrics Enterprise Platform: Dose Management Solution.: Bayer HealthCare (http://www.radiologysolutions.bayer.com/products/ct/dosemanagement/rep/)

Bostani M, McMillan K, DeMarco J J, Cagnon C H and McNitt-Gray M F 2014 Validation of a Monte Carlo model used for simulating tube current modulation in computed tomography over a wide range of phantom conditions/challenges *Med. Phys.* **41** 112101

Chen W, Kolditz D, Beister M, Bohle R and Kalender W A 2012 Fast on-site Monte Carlo tool for dose calculations in CT applications *Med. Phys.* **39** 2985–96

Cristy M and Eckerman K 1987 Specific absorbed fractions of energy at various ages from internal photon sources. I Methods, II one year old, III five year old, IV ten year old, V fifteen year old male and adult female, VI new-born and VII adult male Oak Ridge National Laboratory, Oak Ridge, TN

De González A B *et al* 2009 Projected cancer risks from computed tomographic scans performed in the United States in 2007 *Arch. Intern. Med.* **169** 2071–7

Deak P, Van Straten M, Shrimpton P C, Zankl M and Kalender W A 2008 Validation of a Monte Carlo tool for patient-specific dose simulations in multi-slice computed tomography *Eur. Radiol.* **18** 759–72

DeMarco J *et al* 2005 A Monte Carlo based method to estimate radiation dose from multidetector CT (MDCT): cylindrical and anthropomorphic phantoms *Phys. Med. Biol.* **50** 3989–4004

Ferrero A, Takahashi N, Vrtiska T J, Krambeck A E, Lieske J C and McCollough C H 2019 Understanding, justifying, and optimizing radiation exposure for CT imaging in nephrourology *Nat. Rev. Urol.* **16** 231–44

Fujii K, Nomura K, Muramatsu Y, Obara S, Akahane K and Kusumoto M 2017 Organ dose evaluations based on Monte Carlo simulation for CT examinations using tube current modulation *Radiat. Prot. Dosim.* **174** 387–94

Hardy A J *et al* 2018 Estimating lung, breast, and effective dose from low-dose lung cancer screening CT exams with tube current modulation across a range of patient sizes *Med. Phys.* **45** 4667–82

ICRP 2002 Basic anatomical and physiological data for use in radiological protection: reference values. ICRP Publication 89 *Ann. ICRP* **32** 1–277

IMV Publising 2018 *CT Market Outlook Report* (Arlington, VA: IMV Medical Information Division)

Kalender W A, Saltybaeva N, Kolditz D, Hupfer M, Beister M and Schmidt B 2014 Generating and using patient-specific whole-body models for organ dose estimates in CT with increased accuracy: feasibility and validation *Phys. Med.* **30** 925–33

Lahham A and ALMasri H 2018 Estimation of radiation doses from abdominal computed tomography scans *Radiat. Prot. Dosim.* **182** 235–40

Lee C *et al* 2018 Organ dose estimation accounting for uncertainty for pediatric and young adult CT scans in the United Kingdom *Radiat. Prot. Dosim.* **184** 44–53

Lee M S, Hwang D, Kim J H and Lee J S 2019 Deep-dose: a voxel dose estimation method using deep convolutional neural network for personalized internal dosimetry *Sci. Rep.* **9** 10308

Li X *et al* 2011a Patient-specific radiation dose and cancer risk estimation in CT: Part I. Development and validation of a Monte Carlo program *Med. Phys.* **38** 397–407

Li X *et al* 2011b Patient-specific radiation dose and cancer risk estimation in CT: Part II. Application to patients *Med. Phys.* **38** 408–19

Long D J *et al* 2013 Monte Carlo simulations of adult and pediatric computed tomography exams: validation studies of organ doses with physical phantoms *Med. Phys.* **40** 013901

Muryn J S *et al* 2017 Analysis of uncertainties in Monte Carlo simulated organ and effective dose in chest CT: scanner-and scan-related factors *Phys. Med. Biol.* **62** 3175

Poludniowski G, Landry G, DeBlois F, Evans P and Verhaegen F 2009 SpekCalc: a program to calculate photon spectra from tungsten anode x-ray tubes *Phys. Med. Biol.* **54** N433

Schilham A, van der Molen A J, Prokop M and de Jong H W 2010 Overranging at multisection CT: an underestimated source of excess radiation exposure *Radiographics* **30** 1057–67

Segars W *et al* 2009 Patient specific computerized phantoms to estimate dose in pediatric CT *Proc. SPIE* **7258** 72580H

Siemens AG 2012 *Computed Tomography, SOMATOM Definition Edge, System Owner Manual* (Forchheim/Germany)

Sodickson A *et al* 2009 Recurrent CT, cumulative radiation exposure, and associated radiation-induced cancer risks from CT of adults *Radiology* **251** 175–84

Turner A C *et al* 2010 The feasibility of a scanner-independent technique to estimate organ dose from MDCT scans: Using to account for differences between scanners *Med. Phys.* **37** 1816–25

Waters L S 2002 MCNPX user's manual *Los Alamos National Laboratory*

Xie T, Akhavanallaf A and Zaidi H 2019 Construction of patient-specific computational models for organ dose estimation in radiological imaging *Med. Phys.* **46** 2403–11

Xie T, Poletti P A, Platon A, Becker C D and Zaidi H 2018 Assessment of CT dose to the fetus and pregnant female patient using patient-specific computational models *Eur. Radiol.* **28** 1054–65

Xie T and Zaidi H 2019 Estimation of the radiation dose in pregnancy: an automated patient-specific model using convolutional neural networks *Eur. Radiol.* **29** 6805–15

Yang K, Li X, George Xu X and Liu B 2017 Direct and fast measurement of CT beam filter profiles with simultaneous geometrical calibration *Med. Phys.* **44** 57–70

Zhang G, Ma R, Wang J, He L, Qiu R, Li W and Li J 2019 Preliminary study on automatic organ segmentation using machine learning and application in personalized dosimetry for nuclear medicine *7th Int. Workshop on Computational Human Phantoms (Neuherberg, Germany, 22–24 July 2019)*